Strength and plastic deformation behavior of nanolaminate composites with pre-existing dislocations

Mohsen Damadam[a*], Shuai Shao[b], Iman Salehinia[c], Ioannis Mastorakos[d], Georges Ayoub[e], Hussein M. Zbib[a]

[a] School of Mechanical and Materials Engineering, Washington State University, WA, United States

[b] Department of Mechanical and Industrial Engineering, Louisiana State University, LA, United States

[c] School of Mechanical Engineering, Northern Illinois University, IL, United States

[d] Department of Mechanical and Aeronautical Engineering, Clarkson University, NY, United States

[e] Industrial and Manufacturing Systems Engineering, University of Michigan Dearborn, MI, United States

*Corresponding author, Email: mohsen.damadam@wsu.edu

Abstract

Pre-existing dislocations (PED) are ubiquitous inside crystalline lattices which in turn affect the yield stress and the process of plastic deformation. Hence, understanding the onset of dislocations motion and interaction is critical in modifying or designing new materials with advanced properties so that their mechanical behavior approach realistic conditions. One such family of new materials is the ceramic/metallic nanolaminates. In this work, we have investigated the effect of pre-existing dislocations on the mechanical behavior of NbC/Nb nanolaminates using molecular dynamics simulations. Upon unloading at different strains from stress-strain curve of 3nm NbC/7nm Nb sample, we were able to generate structures with various pre-existing dislocation densities inside the layers. Uniaxial loadings parallel to the interface at two different temperatures ($10K$ and $300K$) were performed on each structure. Also, the yield locus was determined at $300K$ by applying biaxial in-plane loading and fitted with a general flow potential to be used in macroscale analysis. Finally, the tension-compression asymmetry (TCA) was investigated for the structures with pre-existing dislocations along two different in-plane loading directions.

Keywords

Molecular dynamics simulation, Ceramic/metallic multilayer, Nanostructure, Yield surface, Tension-compression asymmetry

1. Introduction

Ceramic/metallic nanolaminate (CMN) composites exhibit high flow strength which is a fraction of theoretical limit, and considerable amount of ductility when the ceramic layer thickness is just a few nano-meters. Combining metals with good ductility and ceramics with high strength and refractory capabilities, leads to novel promising properties and improved performances especially at harsh environments under high pressure and high temperature working conditions. Besides, high corrosion and radiation damage tolerance of CMNs make them unique candidates for coating applications on oil pipelines and nuclear reactors [1–3]. For the above mentioned reasons, the study of the mechanical behavior of CMNs has attracted increasing attention during the recent years [4–6].

Interfaces in nanolaminate composites play an important role in controlling the governing deformation mechanisms and mechanical properties since they act as barriers and sinks to dislocations glide. This role becomes dominant when each individual layer thickness is less than 10 nm due to the very high volume fraction of interfaces [7,8]. In case of coherent interfaces (commensurate) [9] atomic arrangement and slip systems are nearly continuous across the interface [10–12] such that the interface is very strong and allows for dislocation transmission if the coherency stresses (usually of order of GPa), resulting from lattice mismatch, are overcome by the applied stress [13–16]. On the other hand, in semi-coherent interfaces (incommensurate), misfit dislocations are formed on the interface that result in reduced interfacial strengths but stronger barriers for incoming dislocations [11,13,17].

Several studies in the literature are focused on the effect of the individual layer thickness and thickness ratio on the mechanical behavior of CMNs. The results revealed a plastic co-deformation behavior of CMNs when the ceramic layer thickness is less than 5 nm. In fact, although ceramics are brittle, at layer thicknesses below 5 nm, dislocations nucleation has been suggested in the ceramic layer without evidence of cracking [7,18–20]. The transition from brittle to ductile has been attributed to the high resolved shear stress caused by the interaction of the dislocations in the interfaces of the adjoining layers that facilitates dislocation transmission across the interface [21]. Moreover, by decreasing the ceramic layer thickness, the stress field of nucleated dislocations in the softer layer becomes higher than the interfacial shear strength. That in turn results in the shearing of the interface such that dislocation transmission becomes energetically favorable [22,23].

Various experimental and atomistic efforts have studied the deformation mechanisms and mechanical behavior of CMNs under compression and nanoindentation [3,24–26]. The results showed that the strength and hardness increased as the layer thickness decreased. The mechanical behavior of Ti/TiN under compression were shown to have the same trend at different temperatures implying that deformation mechanisms were not temperature dependent. However, the yield stress was shown to be temperature dependent as the shear stress needed for dislocation nucleation was reduced at elevated temperature [27]. Molecular dynamics (MD) simulation of Cu/SiC nanocomposites showed that the deformation mechanisms depend on the interfacial strength and the volume fraction of each phase plays a key role to the mechanical properties [28]. However, the majority of the previous studies examined the structures under uniaxial loading only. The mechanical behavior of CMNs under biaxial in-plane loading has not received much attention so far, even though in the majority of potential applications the structures will operate under biaxial loading. Furthermore, the presence of pre-existing dislocations on the yield surface of CMNs has not been considered so far.

For cases where incipient of plasticity is dominated by the nucleation of dislocations, such as in well-annealed nanocrystalline materials [29–33] where density of pre-existing dislocations are extremely low or in nano multilayers where the activation stress of threader dislocations is high [3,34,35], in previous work [20] we studied the mechanical behavior of NbC/Nb nanocomposites without pre-existing dislocations within the layers using MD simulations. The results from these MD simulations show high yield stresses which correspond to dislocation nucleation. It was

shown that the high stresses are not only due to the typical high strain rates in the MD simulations, which was in turn justified using nucleation theory, but also due to the lack of pre-existing dislocations in the layers which can affect the yield stress and plastic deformation behavior considerably. In this paper, the deformation behavior of single crystal NbC/Nb nanolaminate composites with pre-existing dislocations in the constituent layers is studied under uniaxial tension, uniaxial compression parallel to the interface, and in-plane biaxial loading using molecular dynamics simulations. Two different temperatures are considered with various initial dislocation densities to identify the effect of the dislocation density to the overall deformation behavior. Furthermore, the yield locus of CMNs with pre-existing dislocations at room temperature is obtained and fitted on a general flow potential which allow us to develop a viscoplastic continuum model later on. Finally, the tension-compression yield asymmetry of the CMNs is studied along two different in-plane directions for different initial dislocation densities.

2. Methodology

Molecular dynamics (MD) is a powerful tool to study the physical movement of atoms and their interactions based on Newton's equation of motion [36,37]. The ability to make accurate prediction of material properties by these models is called transferability which is validated with experiment or density functional theory (DFT) calculations [38]. We performed MD simulations on a bilayer NbC/Nb with pre-existing dislocations using LAMMPS [39]. Periodic boundary conditions were applied in x, y, and z directions to mimic the bulk behavior [40]. A second nearest neighbor modified embedded atom method (2NN MEAM) [41,42] interatomic potential was used for both Nb and NbC layer. This potential can accurately reproduce lattice parameters, elastic properties, enthalpy of formation, and surface energies of Nb and NbC [42]. The interface has been oriented according to Baker-Nutting orientation relationship (OR), i.e. $(001)_{NbC} \| (001)_{Nb}$ and $[100]_{NbC} \| [110]_{Nb}$. OVITO package [43] was used for post processing and visualization of atomistic simulation data and centro symmetry parameter (CSP) [44] was used for the visualization of defects.

3. Simulations and Results

Uniaxial tension in the x direction with a constant engineering strain rate of $3 \times 10^8/s$ was applied to the 3nm NbC/7nm Nb nanolaminate with 20.6 nm dimension along both in-plane x and z directions at $10K$ (Fig. 1. red curve). The stress along the other two directions (y and z) was kept zero. Before applying the load, the structure was energetically minimized at $0K$ using the conjugate gradient (CG) method until the configuration potential energy reached less than $1 \times 10^{-10}\ eV$ and then the structure was relaxed at $10K$ for 40 ps employing the isothermal-isobaric (NPT) ensemble [45]. Fig. 1 shows the resulted stress-strain curve. The yield stress is about 14 GPa at a strain of 0.09 in which dislocations started to nucleate and propagate in the Nb layer. By increasing the strain, dislocations began to nucleate in the NbC layer as well at which plastic co-deformation occurred [20]. In order to create structures with pre-existing dislocations, the bilayer nanolaminate was unloaded and relaxed from four different stress states beyond the yield stress as shown in Fig. 1. The loading and unloading process, lead to structures with residual dislocations inside the layers due to the partial elastic recovery. The structures created by unloading from points 1, 2, and 3

contain pre-existing dislocations only inside the Nb layer, while the structure created upon unloading from point 4 consists of pre-existing dislocations in both Nb and NbC layers (Fig. 2).

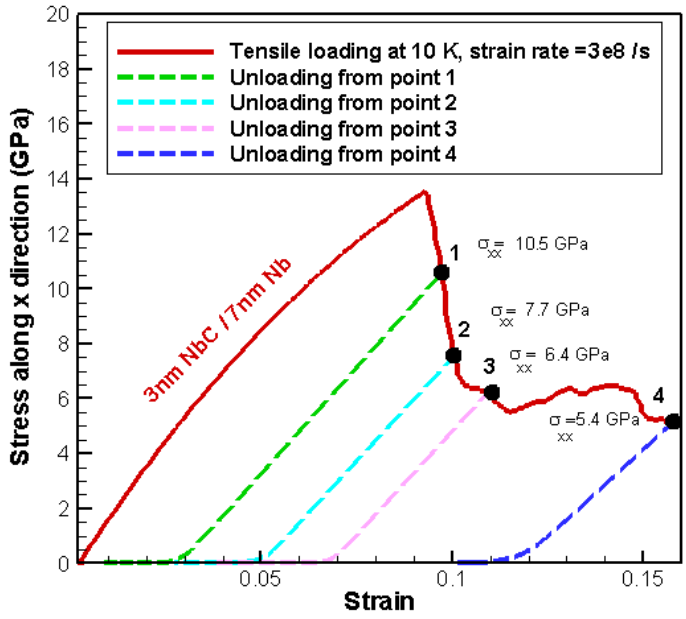

Fig. 1. Stress-strain curve of 3nm NbC/7nm Nb nanolaimate under uniaxial tension parallel to the interface unloaded from four different points with different dislocation densities

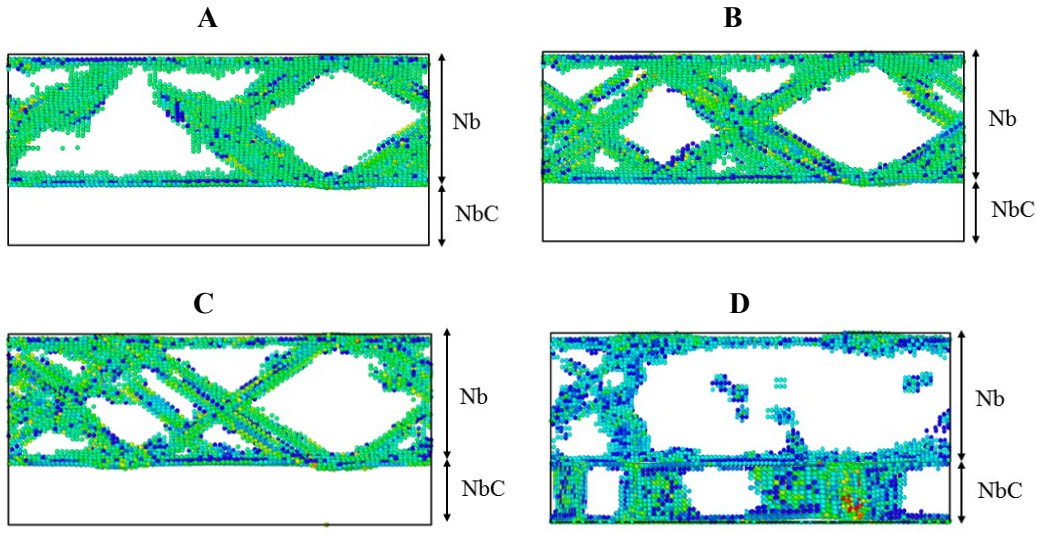

Fig. 2. Structures with pre-existing dislocations created by loading-unloading process at different strains: A, B, C, and D structures above unloaded from points 1, 2, 3, and 4 in Fig. 1 respectively. Total

dislocation length in structures A, B, C, and D is 44527.1Å, 51536Å, 63904.6Å, and 82457.6Å respectively. Snapshots are colored based on *CSP*.

The dislocation density (ρ) is an internal state variable defined as the total dislocation length divided by the unit volume of crystal [46] as:

$$\rho = \frac{l}{V} \tag{1}$$

The centrosymmetry parameter was used to identify the dislocations in the individual layers and interface and the dislocation length was calculated based on the number of atoms and consequently the dislocation density was determined for the 3nm NbC/7nm Nb (red curve) under uniaxial tension as shown in Fig. 3. It can be seen that the dislocation density inside the Nb layer starts increasing at ~56% of the total strain and keeps increasing up to point 3 at which the dislocations interaction is maximum in the Nb layer. Beyond this point, the dislocation density decreases and becomes constant up to point 4 corresponding to 0.16 strain. This is attributed to the high amount of dislocation interactions in the Nb layer that results to a high annihilation rate. Reaching ~78% of the total strain, dislocations start to nucleate in the NbC layer and the dislocation density inside that layer increases up to strain of 0.16 (point 4). For Nb side interface, dislocation density is not zero at zero strain due to the misfit dislocations and then increases upon further deformation tending to approach a constant value as dislocations start crossing into the NbC layer.

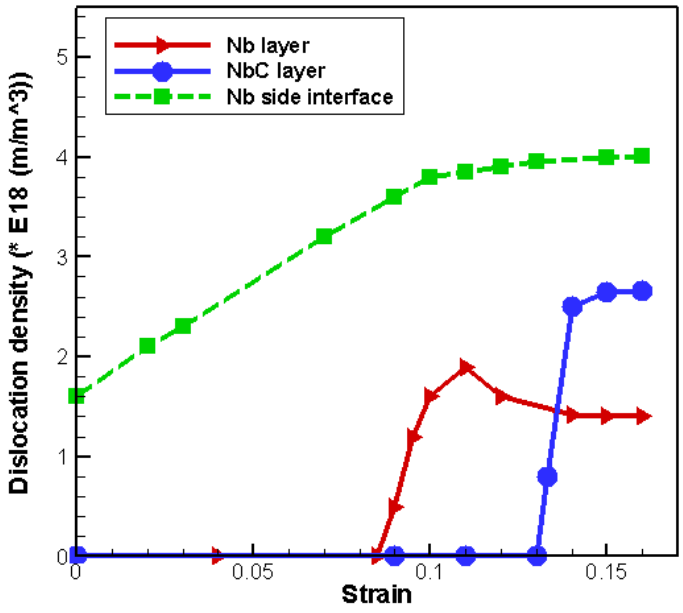

Fig. 3. Dislocation density evolution for 3nm NbC/7nm Nb under uniaxial tension with strain rate of $3 \times 10^8/s$ and temperature $10K$

The structures with pre-existing dislocations have been reloaded under uniaxial tension along x direction by applying constant strain rate of $3 \times 10^8/s$ at two temperatures $10K$ and $300K$. The resulted stress-strain curves are shown in Fig. 4.

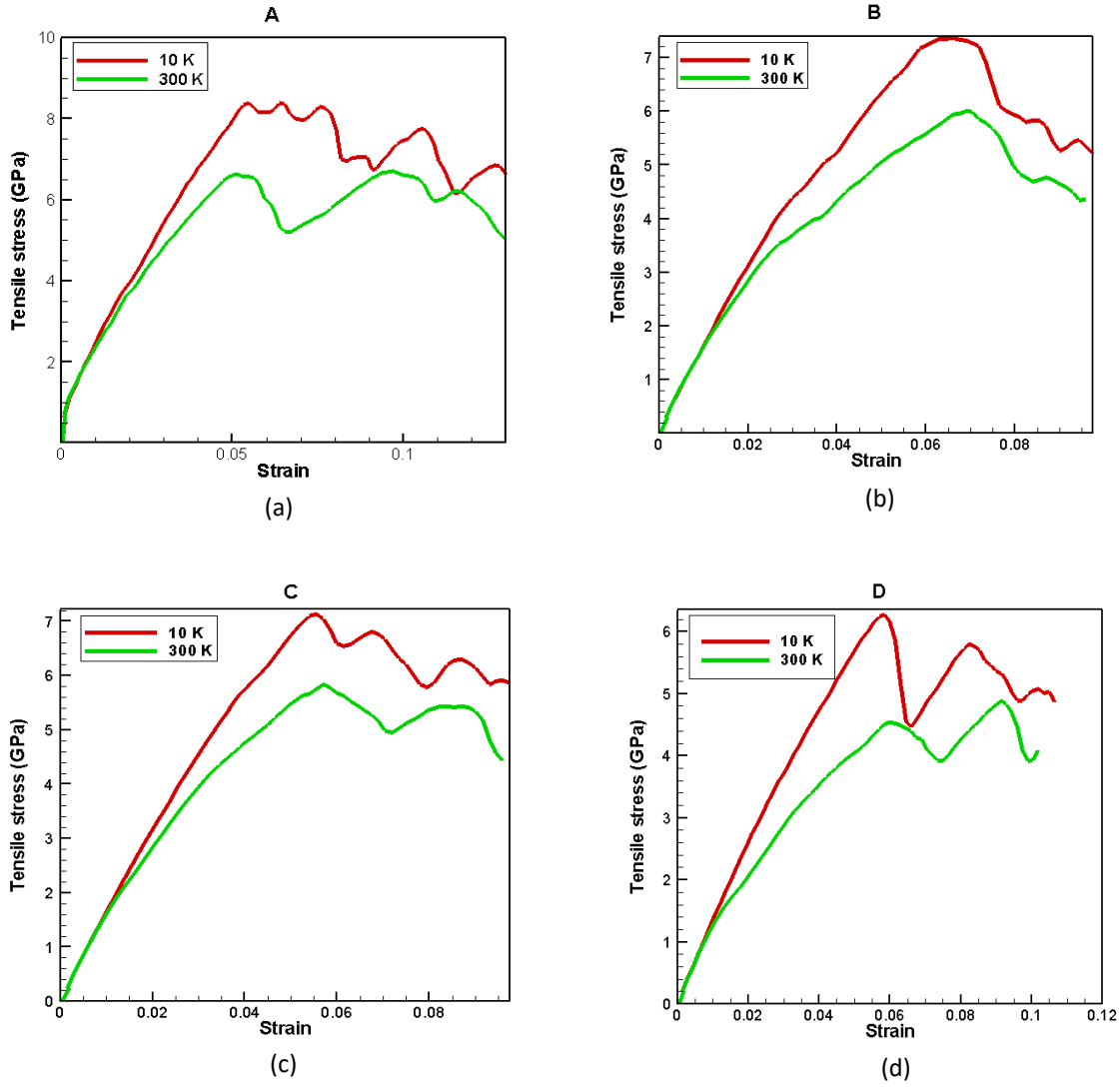

Fig. 4. Tensile stress-strain curves of NbC/Nb structures with pre-existing dislocations created by unloading from point 1 (a), point 2 (b), point 3 (c), and point 4 (d) at $10K$ and $300K$ and constant strain rate $3 \times 10^8/s$.

The results show that the structures with pre-existing dislocations have much lower yield strength compared with the structure without pre-existing dislocations (red curve in Fig. 1).

Furthermore, the yield stress is temperature dependent since the structures loaded at temperature $300K$, exhibit lower yield stress than those loaded at $10K$. Finally, by increasing the initial dislocation content, the yield stress was decreased revealing the importance of loading-unloading history to the mechanical behavior of CMN structures. The total dislocation density in structure D is maximum among all the samples. Fig. 5 shows the variation of yield stress for structures with different initial dislocation density at $10K$ and $300K$.

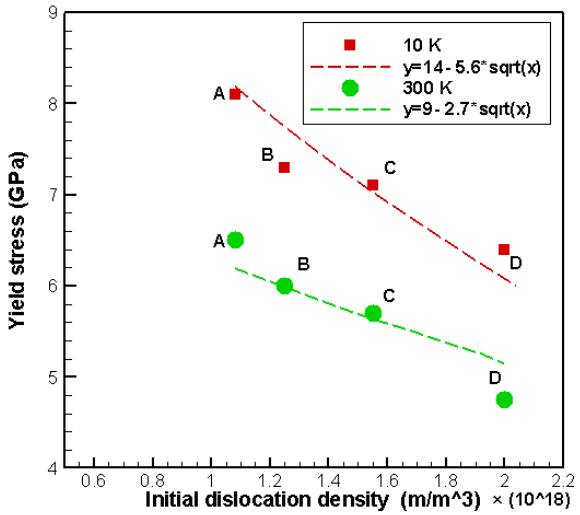

Fig. 5. Yield stress as a function of total initial dislocation density in NbC/Nb bilayer

Yield locus evolution is one of the key features of plastic behavior and it is affected by many factors such as straining direction, strain rate, and temperature [47–49]. In order to determine the yield locus of nanolaminates with pre-existing dislocations, an in-plane non-proportional biaxial loading path including three steps were followed using MD simulations: 1) applying a uniaxial tension or compression with constants strain rate of $3 \times 10^8/s$ along x direction up to a point on the stress-strain curve lower than the yield point; 2) holding the loading at a constant stress level along x direction; 3) applying uniaxial tensile or compressive loading along the z direction using the same constant strain rate until the structure yields. Using this method, and utilizing various combinations of biaxial tension and compression loadings, pair points on the yield locus were determined as shown in Fig. 6.

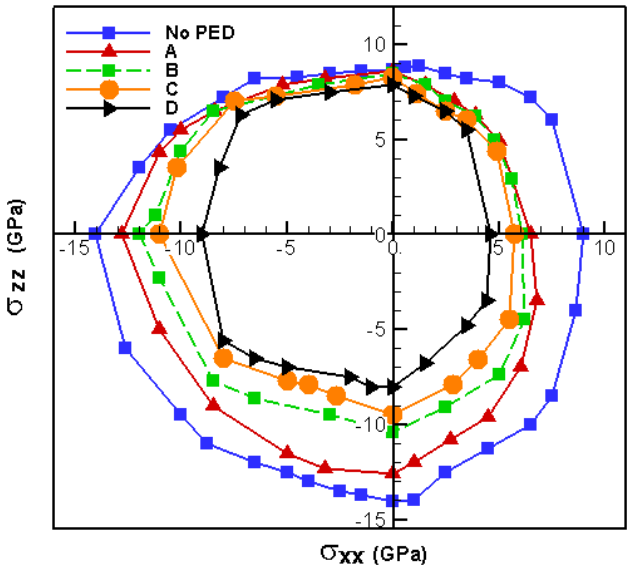

Fig. 6. Evolution of the yield locus of NbC/Nb nanolaminates for structures with different pre-existing dislocations in the layers at 300K

As it is observed in Fig. 5, the yield locus shrinks upon increasing the initial dislocation density in the structure. Furthermore, this effect seems to be less intense during tension along z direction which could be due to the different activated slip systems.

The above results were fitted to an anisotropic function to provide the yield function for the CMNs. The first phenomenological anisotropy yield function was introduced by Hill [50] but his model was not capable of describing the plastic flow of materials with anomalous behavior. For that reason we used the form suggested by Montheillet et al. [51] that has the capability to describe the anisotropic behavior of materials with anomalous behavior in which the yield stress in equi-biaxial loading was higher than the yield stress in uniaxial loading [52,53]. The flow potential is as follows:

$$\emptyset = C|\alpha_1(\sigma_{11} - \sigma_1^*) + \alpha_2(\sigma_{22} - \sigma_2^*)|^m + \alpha_3|(\sigma_{11} - \sigma_1^*) - (\sigma_{22} - \sigma_2^*)|^m - [\sigma_0(\rho_0)]^m \quad (2)$$

where σ_{11} and σ_{22} are the stresses components in the material and the other eight parameters are fitting parameters. After fitting the MD simulations results from Fig. 6 to Eq. (2), one can obtain the plastic flow potential for all the structures. Table. 1 lists the fitting parameters which is observed that scaling factor σ_0 decreases with increasing dislocations density ρ_0 in the NbC/Nb nanolaminate.

Table. 1. Parameters for plastic flow potential based on Eq. (2) fitted with MD results

NbC/Nb	$\rho_0(m/m^3) \times 10^{18}$	C	α_1	σ_1^*(GPa)	α_2	σ_2^*(GPa)	α_3	m	σ_0(GPa)
No PED	0.1	1.4	0.3	-1.8	0.3	-1.99	0.15	1.8	5.8

A	1.1	1.4	0.3	-1.85	0.3	-1.75	0.15	1.8	4.8
B	1.3	1.4	0.3	-1.9	0.3	-1.03	0.15	1.8	4.3
C	1.6	1.4	0.3	-2	0.3	-0.43	0.15	1.8	4.1
D	2.1	1.4	0.3	-2.3	0.3	0.19	0.15	1.8	3.7

Fig. 7 shows the fitting curves based on MD results and Table 1.

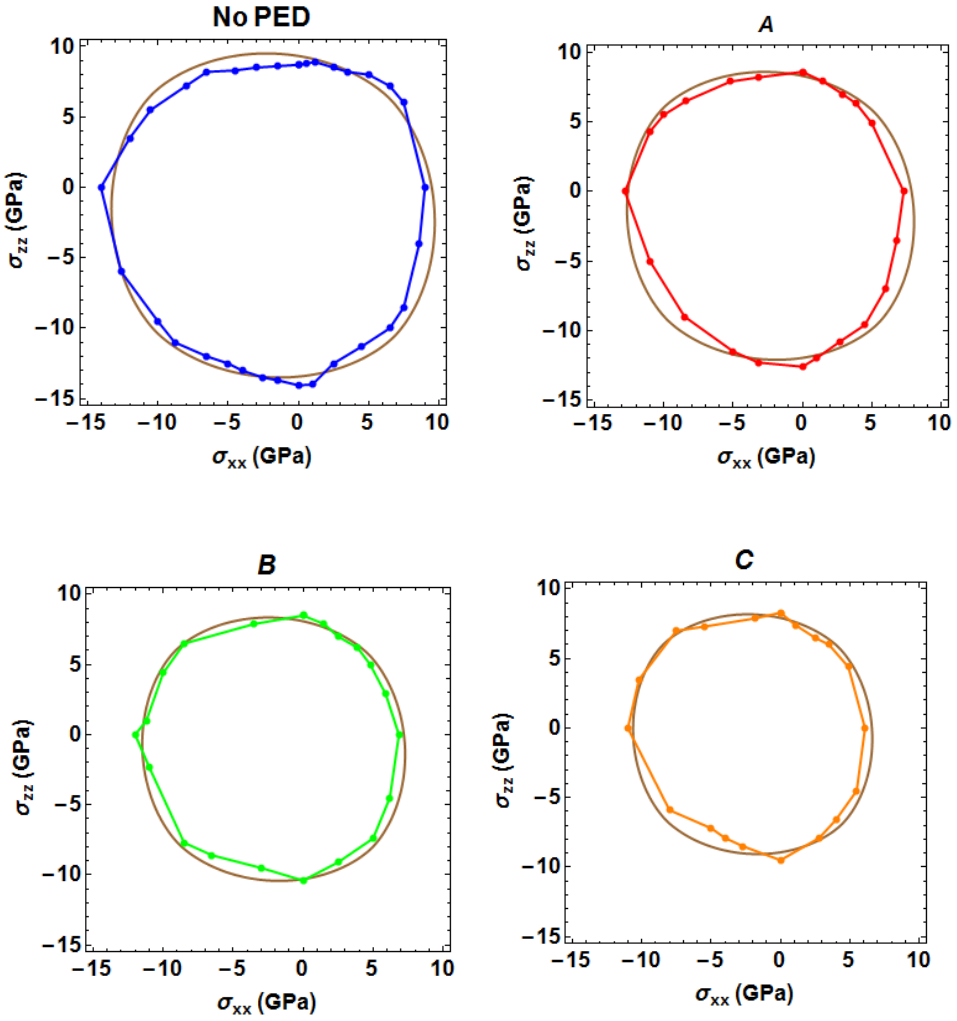

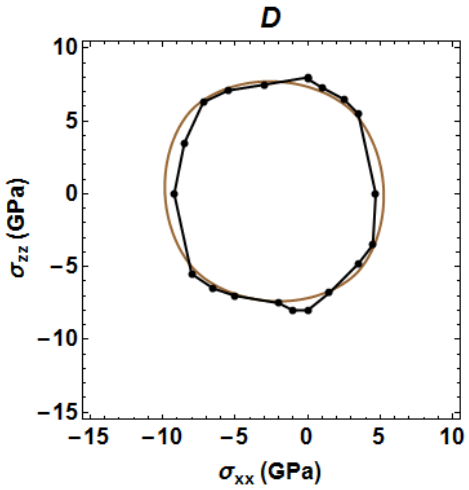

Fig. 7. MD results fitted on the general flow potential for structure with no pre-existing dislocation, structure A, structure B, structure C, and structure D

The observed asymmetry between compression and tension loading is due to the anisotropy of the CMNs. This has also been shown in other atomistic simulation works. For example, in BCC single crystals, atomistic simulations showed that Non-Schmid effects lead to a strong tension-compression asymmetry (TCA) [54,55]. Also for FCC materials, stacking fault tetrahedron (SFT) reduced the TCA and even reversed it for some crystallographic orientations [56]. Compression strength values were found to be higher than the strength in tension for ceramic-metal composites [57]. However, for Al-SiC, results showed that volume fraction of ceramic phase can reverse the TCA of metal-ceramic composites [58]. In general, TCA is defined as the difference in yield stress between tension and compression:

$$TCA = \sigma_Y^t - \sigma_Y^c \tag{3}$$

.

Fig. 8 illustrates the variation of TCA with initial dislocation density for in-plane loading directions.

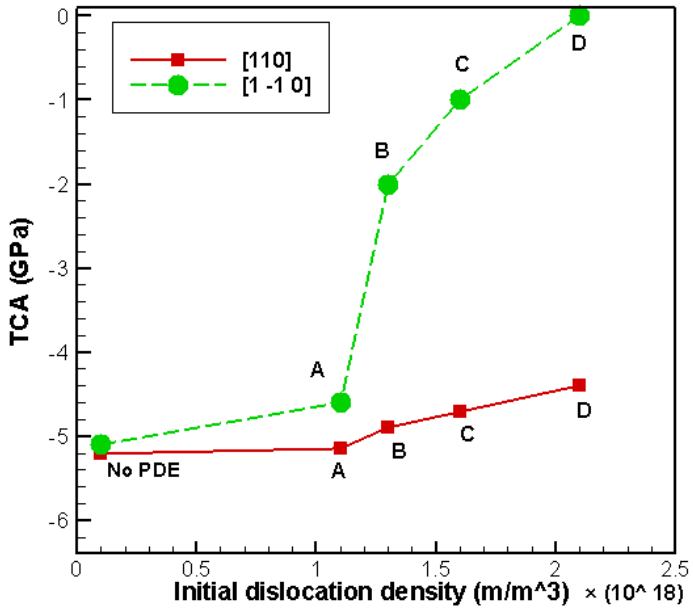

Fig. 8. Variation of TCA with initial dislocation density for [110] and [1-10] directions at 300*K*

As it can be seen in Fig. 8, asymmetry depends on both the direction of applied load and the initial dislocation density. The negative values show that the yield stress is higher in compression than tension. An increase of the initial dislocation density resulted to a decrease in the TCA values along the [110] and [1-10] directions. However, TCA is more sensitive along [1-10] direction. It is noticed that the difference in yield strength between tension and compression along [1-10] direction is almost negligible (TCA~0) for structure D with the highest initial dislocation density among others.

Conclusion

In this work, different NbC/Nb nanolaminates with pre-existing dislocations were created by applying a loading-unloading process. The new structures were reloaded to study their deformation behavior under uniaxial loadings at low temperature and room temperature. Biaxial loading parallel to the x-z plane (interface plane) was applied to the structures with different dislocations densities to find the trend of the yield surfaces evolution at room temperature. Tension-compression yield asymmetry for NbC/Nb bilayer with different initial dislocation densities was also investigated.

The main conclusions from the simulation results are as follows:

1. The presence of pre-existing dislocations decreases the yield strength of NbC/Nb bilayer since pre-existing dislocations facilitate the initiation of plastic flow.
2. Increasing the initial dislocation density shrinks the yield surface.
3. NbC/Nb nanolaminates with pre-existing dislocations are stronger in compression than in tension as predicted by MD results.

4. Tension-compression asymmetry is highly dependent on the loading orientation and initial dislocation density.

Acknowledgment

This work was supported by Qatar National Research Fund (a member of Qatar Foundation) under Grant No. 7-1470-2-528. IM would like to acknowledge the support of National Science Foundation under Grant No. CMMI 1634640. The statements made herein are solely the responsibility of the authors.

References

[1] R. Raghavan, J.M. Wheeler, D. Esqué-de los Ojos, K. Thomas, E. Almandoz, G.G. Fuentes, J. Michler, Mechanical behavior of Cu/TiN multilayers at ambient and elevated temperatures: Stress-assisted diffusion of Cu, Mater. Sci. Eng. A. 620 (2015) 375–382.

[2] S.B. Sinnott, E.C. Dickey, Ceramic/metal interface structures and their relationship to atomic- and meso-scale properties, Mater. Sci. Eng. R Reports. 43 (2003) 1–59.

[3] I. Salehinia, S. Shao, J. Wang, H.M. Zbib, Interface structure and the inception of plasticity in Nb/NbC nanolayered composites, Acta Mater. 86 (2015) 331–340.

[4] C. Mayer, N. Li, N. Mara, N. Chawla, Micromechanical and in situ shear testing of Al–SiC nanolaminate composites in a transmission electron microscope (TEM), Mater. Sci. Eng. A. 621 (2015) 229–235.

[5] S. Huang, J. Wang, C. Zhou, Effect of plastic incompatibility on the strain hardening behavior of Al–TiN nanolayered composites, Mater. Sci. Eng. A. 636 (2015) 430–433.

[6] E.B. Watkins, J. Majewski, J.K. Baldwin, Y. Chen, N. Li, R.G. Hoagland, S.K. Yadav, X.-Y. Liu, I.J. Beyerlein, N.A. Mara, Neutron reflectometry investigations of interfacial structures of Ti/TiN layers deposited by magnetron sputtering, Thin Solid Films. 616 (2016) 399–407.

[7] N.A. Mara, N. Li, A. Misra, J. Wang, Interface-Driven Plasticity in Metal--Ceramic Nanolayered Composites: Direct Validation of Multiscale Deformation Modeling via In Situ Indentation in TEM, JOM. 68 (2016) 143–150.

[8] J. Wang, R.G. Hoagland, A. Misra, Mechanics of nanoscale metallic multilayers: From atomic-scale to micro-scale, Scr. Mater. 60 (2009) 1067–1072.

[9] Y. Chen, S. Shao, X.-Y. Liu, S.K. Yadav, N. Li, N. Mara, J. Wang, Misfit dislocation patterns of Mg-Nb interfaces, Acta Mater. 126 (2017) 552–563.

[10] H.M. Zbib, C.T. Overman, F. Akasheh, D. Bahr, Analysis of plastic deformation in nanoscale metallic multilayers with coherent and incoherent interfaces, Int. J. Plast. 27 (2011) 1618–1639.

[11] R.G. Hoagland, R.J. Kurtz, C.H. Henager, Slip resistance of interfaces and the strength of metallic multilayer composites, Scr. Mater. 50 (2004) 775–779.

[12] I.N. Mastorakos, H.M. Zbib, D.F. Bahr, Deformation mechanisms and strength in

nanoscale multilayer metallic composites with coherent and incoherent interfaces, Appl. Phys. Lett. 94 (2009) 173114.

[13] J. Wang, Q. Zhou, S. Shao, A. Misra, Strength and plasticity of nanolaminated materials, Mater. Res. Lett. 5 (2017) 1–19.

[14] R.G. Hoagland, T.E. Mitchell, J.P. Hirth, H. Kung, On the strengthening effects of interfaces in multilayer fee metallic composites, Philos. Mag. A. 82 (2002) 643–664.

[15] J.P. Hirth, X. Feng, Critical layer thickness for misfit dislocation stability in multilayer structures, J. Appl. Phys. 67 (1990) 3343–3349.

[16] J. Wang, A. Misra, An overview of interface-dominated deformation mechanisms in metallic multilayers, Curr. Opin. Solid State Mater. Sci. 15 (2011) 20–28.

[17] M.R. An, Q. Deng, M.J. Su, H.Y. Song, Y.L. Li, Dependence of deformation mechanisms on layer spacing in multilayered Ti/Al composite, Mater. Sci. Eng. A. 684 (2017) 491–499.

[18] D. Bhattacharyya, N.A. Mara, P. Dickerson, R.G. Hoagland, A. Misra, A transmission electron microscopy study of the deformation behavior underneath nanoindents in nanoscale Al–TiN multilayered composites, Philos. Mag. 90 (2010) 1711–1724.

[19] N. Li, H. Wang, A. Misra, J. Wang, In situ Nanoindentation Study of Plastic Co-deformation in Al-TiN Nanocomposites, Sci. Rep. (2014) 6633.

[20] M. Damadam, S. Shao, I. Salehinia, G. Ayoub, H.M. Zbib, Molecular dynamics simulations of mechanical behavior in nanoscale ceramic–metallic multilayer composites, Mater. Res. Lett. (2017) 1–8.

[21] S. Pathak, N. Li, X. Maeder, R.G. Hoagland, J.K. Baldwin, J. Michler, A. Misra, J. Wang, N.A. Mara, On the origins of hardness of Cu–TiN nanolayered composites, Scr. Mater. 109 (2015) 48–51.

[22] D. Bhattacharyya, N.A. Mara, P. Dickerson, R.G. Hoagland, A. Misra, Compressive flow behavior of Al–TiN multilayers at nanometer scale layer thickness, Acta Mater. 59 (2011) 3804–3816.

[23] J. Wang, R.G. Hoagland, X.Y. Liu, A. Misra, The influence of interface shear strength on the glide dislocation–interface interactions, Acta Mater. 59 (2011) 3164–3173.

[24] I. Salehinia, S. Shao, J. Wang, H.M. Zbib, Plastic Deformation of Metal/Ceramic Nanolayered Composites, JOM. 66 (2014) 2078–2085.

[25] G. Tang, D.R.P. Singh, Y.-L. Shen, N. Chawla, Elastic properties of metal–ceramic nanolaminates measured by nanoindentation, Mater. Sci. Eng. A. 502 (2009) 79–84.

[26] W.M. Mook, R. Raghavan, J.K. Baldwin, D. Frey, J. Michler, N.A. Mara, A. Misra, Indentation Fracture Response of Al–TiN Nanolaminates, Mater. Res. Lett. 1 (2013) 102–108.

[27] W. Yang, G. Ayoub, I. Salehinia, B. Mansoor, H. Zbib, Deformation mechanisms in Ti/TiN multilayer under compressive loading, Acta Mater. 122 (2017) 99–108.

[28] Z. Yang, Z. Lu, T. Wang, Atomistic Simulation of the Mechanical Behaviors of Cu/SiC Nanocomposites, Interface. 2 (2011).

[29] B. Schuh, B. Völker, V. Maier-Kiener, J. Todt, J. Li, A. Hohenwarter, Phase Decomposition of a Single-Phase AlTiVNb High-Entropy Alloy after Severe Plastic Deformation and Annealing, Adv. Eng. Mater. 19 (2017) 1600674--n/a. doi:10.1002/adem.201600674.

[30] O. Renk, A. Hohenwarter, K. Eder, K.S. Kormout, J.M. Cairney, R. Pippan, Increasing the strength of nanocrystalline steels by annealing: Is segregation necessary?, Scr. Mater. 95 (2015) 27–30. doi:http://dx.doi.org/10.1016/j.scriptamat.2014.09.023.

[31] A. V Sergueeva, C. Song, R.Z. Valiev, A.K. Mukherjee, Structure and properties of amorphous and nanocrystalline NiTi prepared by severe plastic deformation and annealing, Mater. Sci. Eng. A. 339 (2003) 159–165. doi:http://dx.doi.org/10.1016/S0921-5093(02)00122-3.

[32] W.W. Gerberich, S.K. Venkataraman, H. Huang, S.E. Harvey, D.L. Kohlstedt, The injection of plasticity by millinewton contacts, Acta Metall. Mater. 43 (1995) 1569–1576.

[33] P. Wo, L. Zuo, A. Ngan, Time-dependent incipient plasticity in Ni 3 Al as observed in nanoindentation, J. Mater. Res. 20 (2005) 489–495.

[34] F. Akasheh, H.M. Zbib, J.P. Hirth, R.G. Hoagland, A. Misra, Interactions between glide dislocations and parallel interfacial dislocations in nanoscale strained layers, J. Appl. Phys. 102 (2007) 34314.

[35] R.L. Schoeppner, J.M. Wheeler, J. Zechner, J. Michler, H.M. Zbib, D.F. Bahr, Coherent Interfaces Increase Strain-Hardening Behavior in Tri-Component Nano-Scale Metallic Multilayer Thin Films, Mater. Res. Lett. 3 (2015) 114–119. doi:10.1080/21663831.2014.995380.

[36] M. Allen, Introduction to molecular dynamics simulation, Comput. Soft Materfrom Synth. Polym. to Proteins. 23 (2004) 1–28.

[37] B.J. Alder, T.E. Wainwright, Studies in Molecular Dynamics. I. General Method, J. Chem. Phys. 31 (1959) 459–466.

[38] N.A. Benedek, A.L.-S. Chua, C. Elsässer, A.P. Sutton, M.W. Finnis, Interatomic potentials for strontium titanate: An assessment of their transferability and comparison with density functional theory, Phys. Rev. B. 78 (2008) 64110.

[39] S. Plimpton, Fast Parallel Algorithms for Short-Range Molecular Dynamics, J. Comput. Phys. 117 (1995) 1–19.

[40] I. Salehinia, J. Wang, D.F. Bahr, H.M. Zbib, Molecular dynamics simulations of plastic deformation in Nb/NbC multilayers, Int. J. Plast. 59 (2014) 119–132.

[41] B.-J. Lee, M.I. Baskes, H. Kim, Y. Koo Cho, Second nearest-neighbor modified embedded atom method potentials for bcc transition metals, Phys. Rev. B. 64 (2001) 184102.

[42] H.-K. Kim, W.-S. Jung, B.-J. Lee, Modified embedded-atom method interatomic potentials for the Nb-C, Nb-N, Fe-Nb-C, and Fe-Nb-N systems, J. Mater. Res. 25 (2010) 1288–1297.

[43] A. Stukowski, Visualization and analysis of atomistic simulation data with OVITO–the Open Visualization Tool, Model. Simul. Mater. Sci. Eng. 18 (2010) 15012.

[44] T. Schneider, E. Stoll, Molecular-dynamics study of a three-dimensional one-component model for distortive phase transitions, Phys. Rev. B. 17 (1978) 1302–1322.

[45] M.E. Tuckerman, J. Alejandre, R. López-Rendón, A.L. Jochim, G.J. Martyna, A Liouville-operator derived measure-preserving integrator for molecular dynamics simulations in the isothermal–isobaric ensemble, J. Phys. A. Math. Gen. 39 (2006) 5629.

[46] D. Hull, D. Bacon, Introduction to Dislocations, Butterworth-Heinemann, 2001.

[47] A. Phillips, T. Juh-Ling, The effect of loading path on the yield surface at elevated temperatures, Int. J. Solids Struct. 8 (1972) 463–474.

[48] A. Phillips, J.-L. Tang, M. Ricciuti, Some new observations on yield surfaces, Acta Mech. 20 (1974) 23–39.

[49] T. Naka, T. Uemori, R. Hino, M. Kohzu, K. Higashi, F. Yoshida, Effects of strain rate, temperature and sheet thickness on yield locus of AZ31 magnesium alloy sheet, J. Mater. Process. Technol. 201 (2008) 395–400.

[50] R. Hill, Theoretical plasticity of textured aggregates, in: Math. Proc. Cambridge Philos. Soc., Cambridge University Press, 1979.

[51] F. Montheillet, J.J. Jonas, M. Benferrah, Development of anisotropy during the cold rolling of aluminium sheet, Int. J. Mech. Sci. 33 (1991) 197–209.

[52] J. Woodthorpe, R. Pearce, The anomalous behaviour of aluminium sheet under balanced biaxial tension, Int. J. Mech. Sci. 12 (1970) 341–347.

[53] W. Hu, Characterized behaviors and corresponding yield criterion of anisotropic sheet metals, Mater. Sci. Eng. A. 345 (2003) 139–144.

[54] Z.Q. Wang, I.J. Beyerlein, An atomistically-informed dislocation dynamics model for the plastic anisotropy and tension–compression asymmetry of BCC metals, Int. J. Plast. 27 (2011) 1471–1484.

[55] A. Patra, T. Zhu, D.L. McDowell, Constitutive equations for modeling non-Schmid effects in single crystal bcc-Fe at low and ambient temperatures, Int. J. Plast. 59 (2014) 1–14.

[56] I. Salehinia, D.F. Bahr, Crystal orientation effect on dislocation nucleation and multiplication in FCC single crystal under uniaxial loading, Int. J. Plast. 52 (2014) 133–146.

[57] V. Tomar, M. Zhou, Tension-compression strength asymmetry of nanocrystalline α-Fe2O3+fcc-Al ceramic-metal composites, Appl. Phys. Lett. 88 (2006) 233107.

[58] A.M. Dongare, B. LaMattina, A.M. Rajendran, Strengthening Behavior and Tension–

Compression Strength–Asymmetry in Nanocrystalline Metal–Ceramic Composites, J. Eng. Mater. Technol. 134 (2012) 41003–41008.